IRE1 directs proteasomal and lysosomal degradation of misfolded rhodopsin

Wei-Chieh Chiang, Carissa Messah, and Jonathan H. Lin
Department of Pathology, University of California, San Diego, La Jolla, CA 92093

ABSTRACT **Endoplasmic reticulum (ER) is responsible for folding of secreted and membrane proteins in eukaryotic cells. Disruption of ER protein folding leads to ER stress. Chronic ER stress can cause cell death and is proposed to underlie the pathogenesis of many human diseases. Inositol-requiring enzyme 1 (IRE1) directs a key unfolded protein response signaling pathway that controls the fidelity of ER protein folding. IRE1 signaling may be particularly helpful in preventing chronic ER stress and cell injury by alleviating protein misfolding in the ER. To examine this, we used a chemical-genetic approach to selectively activate IRE1 in mammalian cells and tested how artificial IRE1 signaling affected the fate of misfolded P23H rhodopsin linked to photoreceptor cell death. We found that IRE1 signaling robustly promoted the degradation of misfolded P23H rhodopsin without affecting its wild-type counterpart. We also found that IRE1 used both proteasomal and lysosomal degradation pathways to remove P23H rhodopsin. Surprisingly, when one degradation pathway was compromised, IRE1 signaling could still promote misfolded rhodopsin degradation using the remaining pathway. Last, we showed that IRE1 signaling also reduced levels of several other misfolded rhodopsins with lesser effects on misfolded cystic fibrosis transmembrane conductance regulator. Our findings reveal the diversity of proteolytic mechanisms used by IRE1 to eliminate misfolded rhodopsin.**

Monitoring Editor
Jeffrey L. Brodsky
University of Pittsburgh

Received: Aug 2, 2011
Revised: Nov 21, 2011
Accepted: Dec 28, 2011

INTRODUCTION

Eukaryotic cells respond to protein misfolding in the endoplasmic reticulum (ER) by activating intracellular signaling pathways, collectively termed the unfolded protein response (UPR). Inositol-requiring enzyme 1 (IRE1) encodes an ER-resident transmembrane protein that controls the most highly conserved UPR signaling pathway (Hetz and Glimcher, 2009). IRE1 bears a luminal domain that monitors the fidelity of protein folding within the ER coupled to cytosolic kinase and endoribonuclease (RNase) domains (Ron and Walter, 2007). In response to protein misfolding in the ER, IRE1 undergoes oligomerization and activation of its kinase and RNase functions that then initiate the nonconventional splicing of *Xbp-1* mRNA (Cox *et al.*, 1993; Gonzalez *et al.*, 1999; Yoshida *et al.*, 2001; Calfon *et al.*, 2002). Spliced *Xbp-1* mRNA encodes a transcription activator that upregulates target genes, including ER chaperones and protein-folding enzymes, ER structural and transport proteins, and ER-associated degradation (ERAD) components (Lee *et al.*, 2003). IRE1 signaling through the production of spliced X-box-binding protein 1 (XBP-1) transcription factor thereby enhances the protein folding environment of the ER by expanding the amount of ER and its constituent protein-folding machineries, as well as clearing misfolded ER proteins by targeting them for degradation through ERAD. In response to strong ER stress, IRE1 signaling also causes regulated IRE1-dependent mRNA decay (RIDD) and Jun N-terminal kinase (JNK) activation (Urano *et al.*, 2000; Hollien and Weissman, 2006; Hollien *et al.*, 2009; Oikawa *et al.*, 2007). Many cells and tissues lacking IRE1 show profound defects in the generation of secreted and membrane proteins and undergo cell death (Zhang *et al.*, 2005, 2011; Iwawaki *et al.*, 2010), underscoring the importance of IRE1 in regulating ER protein folding and homeostasis.

This article was published online ahead of print in MBoC in Press (http://www.molbiolcell.org/cgi/doi/10.1091/mbc.E11-08-0663) on January 4, 2012.

Address correspondence to: Jonathan H. Lin (jlin@ucsd.edu).

Abbreviations used: 1NM-PP1, 4-amino-1-*tert*-butyl-3-(1′-naphthylmethyl) pyrazolo[3,4-*d*]pyrimidine; BiP, immunoglobulin-binding protein; CFTR, cystic fibrosis transmembrane conductance regulator; EDEM1, ER-degradation enhancing α-mannosidase-like protein 1; ER, endoplasmic reticulum; ERAD, ER-associated protein degradation; GAPDH, glyceraldehyde 3-phosphate dehydrogenase; GFP, green fluorescent protein; IRE1, inositol-requiring enzyme 1; PERK, PKR-like endoplasmic reticulum kinase; UPR, unfolded protein response; XBP-1, X-box-binding protein 1.

Rhodopsin is a member of the G-protein–coupled receptor superfamily of membrane proteins that is expressed exclusively and robustly by photoreceptor cells in the eye in mammals, where it comprises >90% of all proteins in the photoreceptor outer segment disk membranes (Hargrave, 2001). Rhodopsin plays an essential role in vision by initiating the visual signal transduction cascade in the photoreceptor outer segment in response to light. More than 100 distinct mutations in *rhodopsin* have been identified that cause photoreceptor cell death and vision loss in autosomal-dominant forms of retinitis pigmentosa (RetNet—Retinal Information Network, www.sph.uth.tmc.edu/Retnet). Wild-type rhodopsin is normally synthesized and folded in the ER prior to delivery to the outer segment. By contrast, many mutant rhodopsins are defective in their folding and retained within the ER, where they cause ER stress and ultimately photoreceptor cell death (Sung *et al.*, 1991; Kaushal and Khorana, 1994; Illing *et al.*, 2002; Saliba *et al.*, 2002; Lin *et al.*, 2007; Gorbatyuk *et al.*, 2010). Chemical and genetic chaperones have shown partial efficacy in restoring mutant rhodopsin protein folding, delivery out of the ER, and improving retinal function (Noorwez *et al.*, 2003, 2004, 2009; Mendes and Cheetham, 2008; Kosmaoglou *et al.*, 2009; Gorbatyuk *et al.*, 2010). Alternatively, ribozyme-mediated degradation of *P23H rhodopsin* mRNA that spared wild-type *rhodopsin* has also shown efficacy in enhancing photoreceptor cell survival in transgenic animals expressing mutant and wild-type rhodopsins (Lewin *et al.*, 1998; LaVail *et al.*, 2000). Therefore finding mechanisms that enhance mutant rhodopsin folding or selectively remove mutant rhodopsin might offer new approaches to promote the survival of photoreceptors that are confronted with misfolded rhodopsin and ER stress.

Given IRE1's fundamental role in regulating ER function, we hypothesized that IRE1 activity might promote the folding and/or removal of misfolded proteins linked to disease such as mutant rhodopsins. To test this, we used a chemical-genetic strategy that enabled selective activation of IRE1's RNase function by the cell permeable small molecule 4-amino-1-*tert*-butyl-3-(1′-naphthylmethyl) pyrazolo[3,4-*d*]pyrimidine (1NM-PP1; Bishop *et al.*, 2000). We previously showed that this system promoted robust splicing of *Xbp-1* by IRE1 in the presence of 1NM-PP1 (Lin *et al.*, 2007, 2009; Hollien *et al.*, 2009). Of importance, this chemical-genetic system did not activate other UPR signaling pathways controlled by protein kinase RNA-like endoplasmic reticulum kinase (PERK) and activating transcription factor 6 (ATF6), did not activate RIDD or JNK, and did not cause apoptosis (Lin *et al.*, 2007, 2009; Hollien *et al.*, 2009). Here we used this approach to determine how selective activation of IRE1's RNase affected the fate of mutant rhodopsins and other misfolded proteins in mammalian cells.

RESULTS

ER stress reduces levels of wild-type and misfolded membrane proteins.

We focused on mutant rhodopsin bearing a proline-to-histidine missense mutation at amino acid residue 23 (P23H). The P23H rhodopsin mutation was first identified in families with autosomal-dominant retinitis pigmentosa (Dryja *et al.*, 1990) and also caused photoreceptor cell death in mammalian models of retinal degeneration when expressed singly or as multicopy transgenes (Olsson *et al.*, 1992; Lin *et al.*, 2007; Sakami *et al.*, 2011). Wild-type rhodopsin normally folds and undergoes N-linked glycosylation in the ER prior to export to the photoreceptor rod outer segment (Sung *et al.*, 1991; Illing *et al.*, 2002). These features are recapitulated in cell culture, where wild-type rhodopsin migrated predominantly as a diffuse 39- to 50-kDa molecular band on SDS gels and Western blot analysis corresponding to glycosylated monomeric rhodopsin and was efficiently exported from ER and localized at the plasma membrane (Figure 1, A and B, left). By contrast, mutant P23H rhodopsin protein primarily formed dimers and multimeric aggregates and was retained within the ER (Figure 1, A and B, right).

First, we examined how activation of all UPR pathways including IRE1 affected P23H rhodopsin protein. We found sharps drop in P23H rhodopsin protein levels upon addition of tunicamycin (TM), an agent that blocks N-linked glycosylation, or thapsigargin (TG), an agent that blocks sarco/endoplasmic reticulum Ca^{2+} ATPase, to the medium of cells expressing P23H rhodopsin (Supplemental Figure S1A; reduced to 28% of levels in untreated cells by TM and 52% of levels in untreated cells by TG). This reduction in protein levels showed no specificity for P23H rhodopsin. Activation of UPR by TM or TG also caused sharp drops in the levels of wild-type rhodopsin protein (Supplemental Figure S1B; reduced to 67% of levels in untreated cells by TM and 33% of levels in untreated cells by TG) and another membrane protein, vascular cell adhesion molecule 1 (VCAM-1; Supplemental Figure S1C; reduced to 15% by TM and 17% by TG) in analogous experiments, even though neither protein bore missense misfolding mutations. This drop in levels of correctly folded proteins, as well as misfolded P23H rhodopsin, was consistent with the global translational attenuation observed after activation of the PERK branch of the UPR, concomitant with IRE1 activation, seen upon imposition of ER stress by these agents (Harding *et al.*, 1999).

IRE1 selectively reduces levels of misfolded P23H rhodopsin

Next we examined how selective activation of IRE1 signaling affected P23H rhodopsin protein. When we expressed P23H rhodopsin in cells stably expressing IRE1[I642G], a genetically modified form of human IRE1 whose RNase activity can be toggled on/off by 1NM-PP1 without activating other UPR signaling pathways (Lin *et al.*, 2007, 2009), we observed a sharp drop in P23H rhodopsin protein with addition of 1NM-PP1 compared with untreated cells (Figure 2A; down to ~46% of protein levels in untreated cells by 24 h of drug exposure). This drop in P23H rhodopsin levels was highly specific for the misfolded protein, as wild-type rhodopsin protein levels showed minimal changes in analogous experiments (Figure 2B). Furthermore, this drop in P23H rhodopsin levels specifically required IRE1[I642G] because P23H rhodopsin protein levels were unchanged when 1NM-PP1 was added to wild-type HEK293 cells lacking IRE1[I642G] (Supplemental Figure S2).

P23H rhodopsin is highly prone to form detergent-insoluble aggregates (Illing *et al.*, 2002). Therefore we examined in more detail which species of P23H rhodopsin (detergent soluble or insoluble) was affected by IRE1 signaling. When we examined levels of P23H rhodopsin protein in 1% NP-40 soluble supernatant compared with detergent-insoluble pellet fractions, we found that the drop in P23H rhodopsin protein levels occurred almost entirely with the P23H rhodopsin present in the detergent-insoluble fraction after IRE1 activation by 1NM-PP1 (Figure 3A). Furthermore, we observed this selective drop in detergent-insoluble pellet fractions of P23H rhodopsin across a wide range of detergents, including 1% Triton X-100, 1% dodecyl-β-D-maltoside (DM), 1% Triton X-114, and 1% digitonin (Figure 3A). To rule out the possibility that selective IRE1 induction shifted the insoluble material into a form that was not reactive to 1D4 anti-rhodopsin antibody, recognizing the C-terminus of rhodopsin, we used a different rhodopsin antibody recognizing the N-terminus of rhodopsin, B630N anti-rhodopsin antibody. The selective drop in detergent-insoluble pellet fractions of P23H rhodopsin was also observed (Supplemental Figure S3). Taken together, our

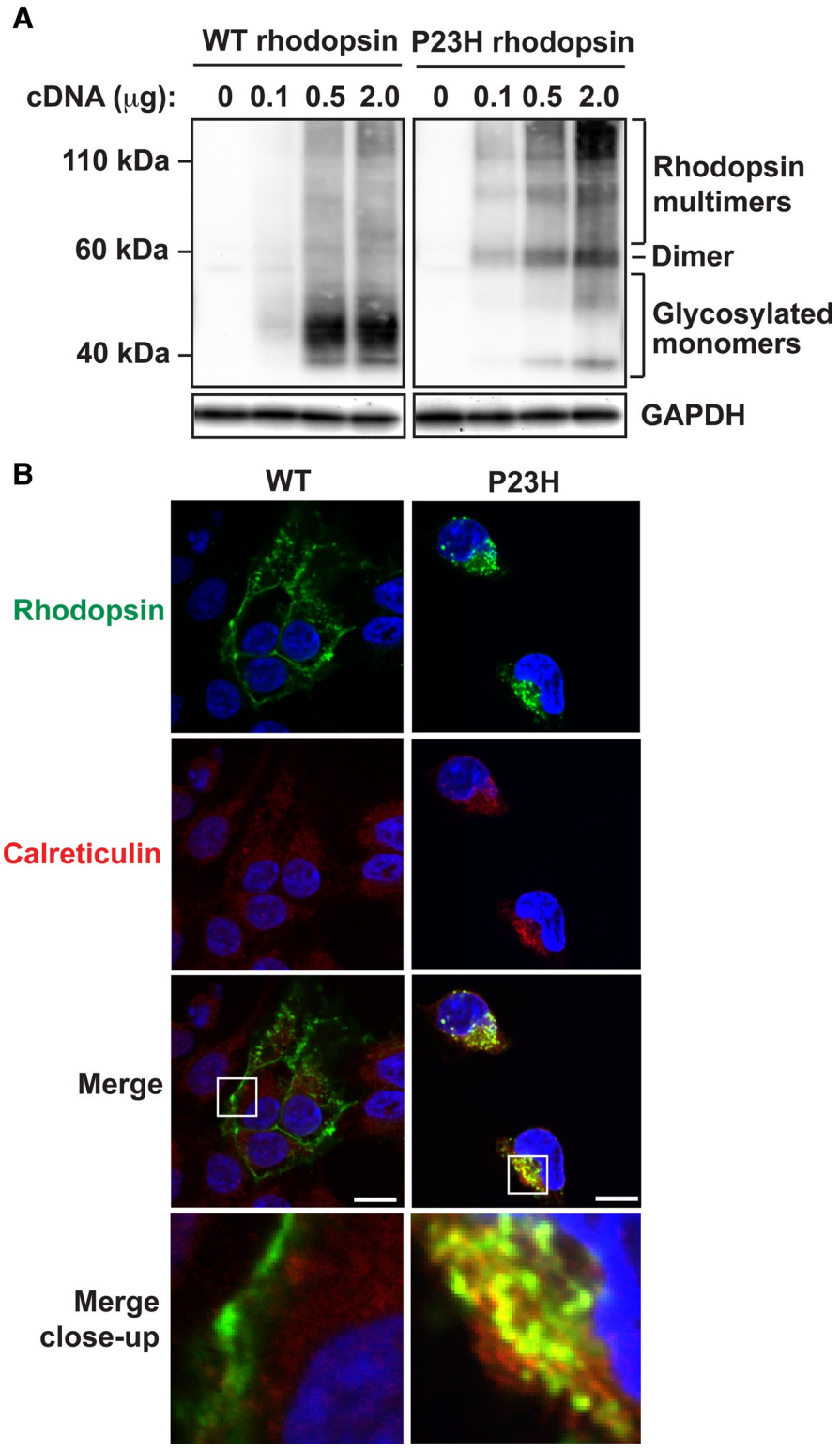

FIGURE 1: Cellular and molecular defects induced by the P23H missense mutation in rhodopsin. (A) Wild-type or P23H rhodopsin cDNA was expressed in HEK293 cells as indicated, and rhodopsin protein levels and mobility were detected by SDS–PAGE separation and immunoblotting. GAPDH levels were assessed as a protein loading control. Positions of glycosylated monomeric, dimeric, and multimeric rhodopsin protein species are as indicated. (B) A 0.1-μg amount of wild-type or P23H rhodopsin cDNA was expressed in HEK293 cells, and the subcellular localization of rhodopsin was visualized by immunofluorescence labeling and confocal microscopy (shown in green). The endoplasmic reticulum was visualized by calreticulin immunostaining (shown in red). The nucleus was visualized by DAPI staining (shown in blue). Magnification bars, 10 μm.

findings demonstrated that IRE1 signaling dramatically reduced misfolded P23H rhodopsin protein levels in cells, with minimal changes to the levels of its wild-type rhodopsin protein counterpart. Furthermore, IRE1 signaling selectively reduced levels of P23H rhodopsin protein in insoluble pellet forms, with minimal changes on levels of P23H rhodopsin in the soluble supernatant fraction.

IRE1 promotes P23H rhodopsin protein degradation

Next we investigated how IRE1 caused the sharp drop seen in levels of P23H rhodopsin protein. Spliced XBP-1 protein transcriptionally upregulates a broad range of chaperones and enzymes that promote ERAD (Lee *et al.*, 2003), and overexpression of ER-degradation enhancing α-mannosidase-like protein 1 (EDEM1), a lectin involved in ERAD (Yoshida *et al.*, 2003; Eriksson *et al.*, 2004; Olivari *et al.*, 2005), has been shown to promote P23H rhodopsin protein degradation and enhance its delivery to membrane (Kosmaoglou *et al.*, 2009). Therefore we investigated how IRE1 signaling affected P23H rhodopsin protein stability and degradation. Because the form of P23H rhodopsin protein most sensitive to IRE1 signaling was insoluble in detergents used for immunoprecipitation and metabolic labeling studies (Figure 3A and Supplemental Figure S3), we were unable to perform pulse-chase analysis to accurately measure how IRE1 signaling affected P23H rhodopsin protein half-life. Instead, we devised a strategy to measure the changes in P23H rhodopsin protein stability in response to IRE1 signaling by creating a cell line stably expressing both tetracycline-inducible P23H rhodopsin and IRE1[I642G]. In this system, P23H rhodopsin protein synthesis required the presence of doxycycline, and its synthesis could be induced with no toxicity for up to 10 d in vitro. When doxycycline was removed, *P23H rhodopsin* transcription ceased, and the remaining pool of P23H rhodopsin protein was eliminated via endogenous protein turnover. IRE1[I642G]'s ability to splice *Xbp-1* after 1NM-PP1 addition was not changed in these cells (Supplemental Figure S4). Using this system, we briefly induced the expression of P23H rhodopsin protein by the addition of doxycycline. Doxycycline was then removed from media, and when *P23H rhodopsin* mRNA levels had returned to basal minimal levels, we activated IRE1 signaling by adding 1NM-PP1 for another 24 h. Under these conditions, we saw a pronounced decrease in the remaining pool of P23H rhodopsin protein with addition of 1NM-PP1 compared with untreated cells (Figure 3B; down to 27% of protein levels in untreated cells). These changes in P23H rhodopsin protein levels most likely arose from degradation,

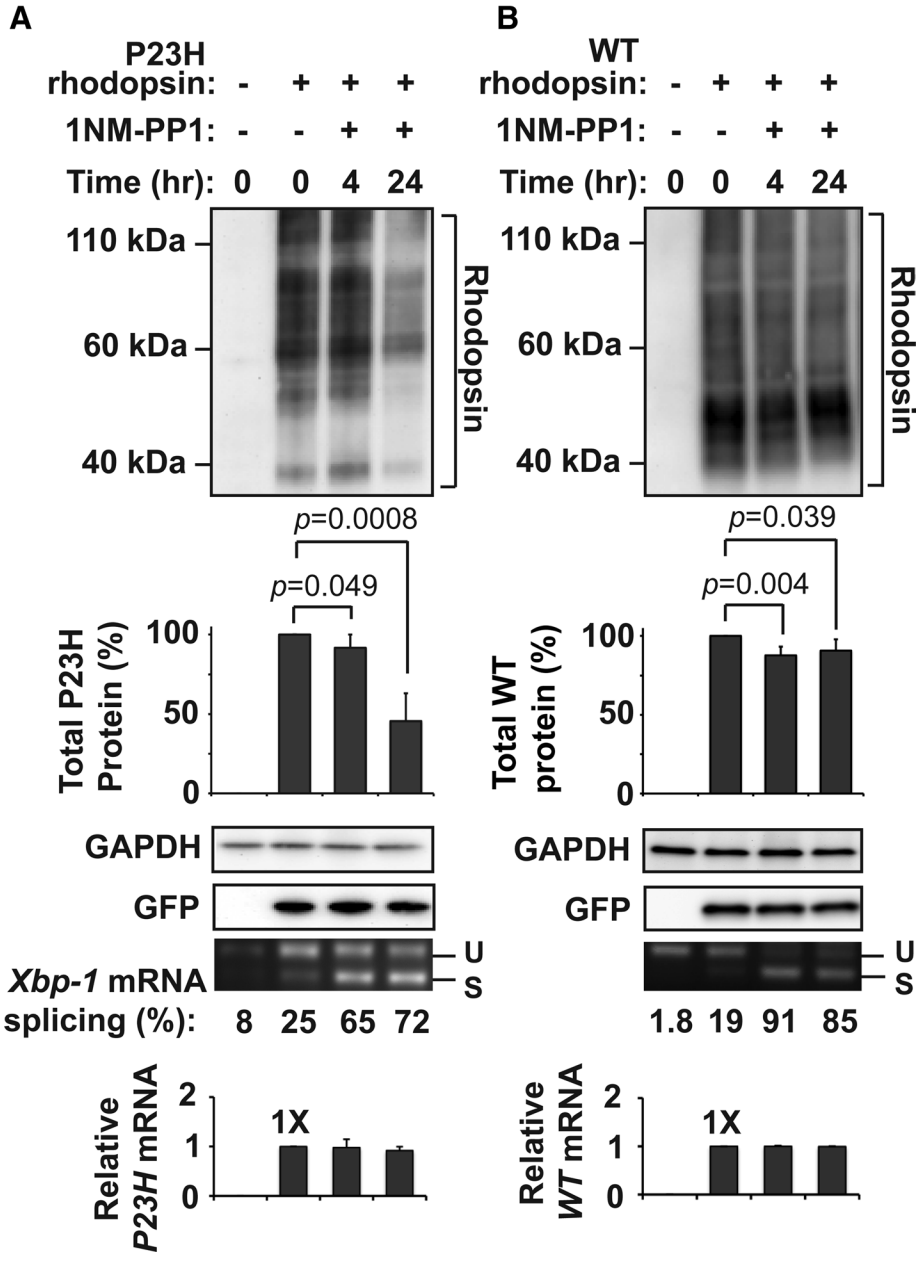

FIGURE 2: IRE1 selectively decreases levels of P23H rhodopsin protein. (A) P23H rhodopsin was expressed in HEK293 cells bearing IRE1[I642G], and 1NM-PP1 (5 μM) was applied for the indicated durations. (B) Wild-type rhodopsin was expressed in HEK293 cells bearing IRE1[I642G], and 1NM-PP1 (5 μM) was applied as indicated. (A, B) Total rhodopsin protein levels were detected by immunoblotting and quantified. GAPDH levels were assessed as a protein loading control. Cotransfected GFP levels were assessed to control for transfection efficiency. *Xbp-1* mRNA splicing was assessed by reverse transcription-PCR, and the amount of spliced *Xbp-1* mRNA was quantified as a percentage of the total amounts of unspliced (u) and spliced (s) amplicons. *P23H* and wild-type *rhodopsin* mRNA levels were measured by real-time PCR and are expressed relative to levels in cells that were not treated with 1NM-PP1. Immunoblots are representative of three independent experiments. Error bars represent SDs from three experiments. The p values were determined by Student's *t* test analysis.

as there was minimal *P23H rhodopsin* mRNA and therefore little, if any, new P23H rhodopsin protein being synthesized under these conditions without doxycycline. These results provided evidence that IRE1 signaling directly and robustly promoted the degradation of P23H rhodopsin protein.

IRE1's RIDD activity also cleaves ER-targeted mRNAs, leading to drops in levels of some membrane and secreted proteins (Han *et al.*, 2009; Hollien *et al.*, 2009). Previous studies showed that 1NM-PP1 promotes *Xbp-1* splicing by IRE1[I642G]'s RNase without activating RIDD (Hollien *et al.*, 2009). Consistent with those findings, we observed robust *Xbp-1* mRNA splicing without changes in *P23H rhodopsin* mRNA transcript levels after addition of 1NM-PP1 (Figure 2, A and B, bottom). These findings indicated that the drop in P23H rhodopsin protein levels seen after IRE1[I642G] activation did not arise from loss of transcription or decay of the *P23H rhodopsin* mRNA.

Proteasome and lysosome degrade P23H rhodopsin

We next explored the proteolytic mechanisms responsible for degrading P23H rhodopsin. Similar to prior studies, we observed a significant increase in P23H rhodopsin protein levels, in both soluble and pellet fractions, after addition of proteasome inhibitors, lactacystin, or MG-132 (Figure 4A and 4B, top, and Supplemental Figure S5), indicating a role for the proteasome in P23H rhodopsin protein degradation (Illing *et al.*, 2002; Saliba *et al.*, 2002). However, to our surprise, when we activated IRE1 signaling with 1NM-PP1 in the presence of proteasome inhibitors, total P23H rhodopsin protein levels still decreased, dropping from ~240 to ~140% of untreated levels after IRE1 activation in the presence of lactacystin or MG-132 (Figure 4, A and B). We saw similar findings when we examined soluble and pellet fractions of P23H rhodopsin treated with lactacystin and 1NM-PP1 (Supplemental Figure S5). We confirmed that lactacystin and MG-132 remained effective in these studies by demonstrating increased protein levels of GFPu, an unstable variant of green fluorescent protein (GFP) previously used as a reporter of proteasome activity (Bence *et al.*, 2001; Supplemental Figure S6). We also confirmed that 1NM-PP1 remained effective in activating IRE1[I642G]'s RNase activity under conditions of proteasome inhibition by demonstrating robust *Xbp-1* mRNA splicing after addition of lactacystin or MG-132 (Supplemental Figure S7, A and B). Taken together, our findings indicated that P23H rhodopsin protein degradation depended upon proteasome function, but, of interest, our findings suggested that additional proteolytic mechanisms cleared P23H rhodopsin after IRE1 activation.

Besides the proteasome, the autophagy–lysosome system is another cellular mechanism that degrades proteins, and rapamycin was previously reported to promote P23H rhodopsin degradation via induction of autophagy (Kaushal, 2006). When we expressed P23H rhodopsin in cells, we saw increased colocalization between P23H rhodopsin and lysosomal-associated membrane protein

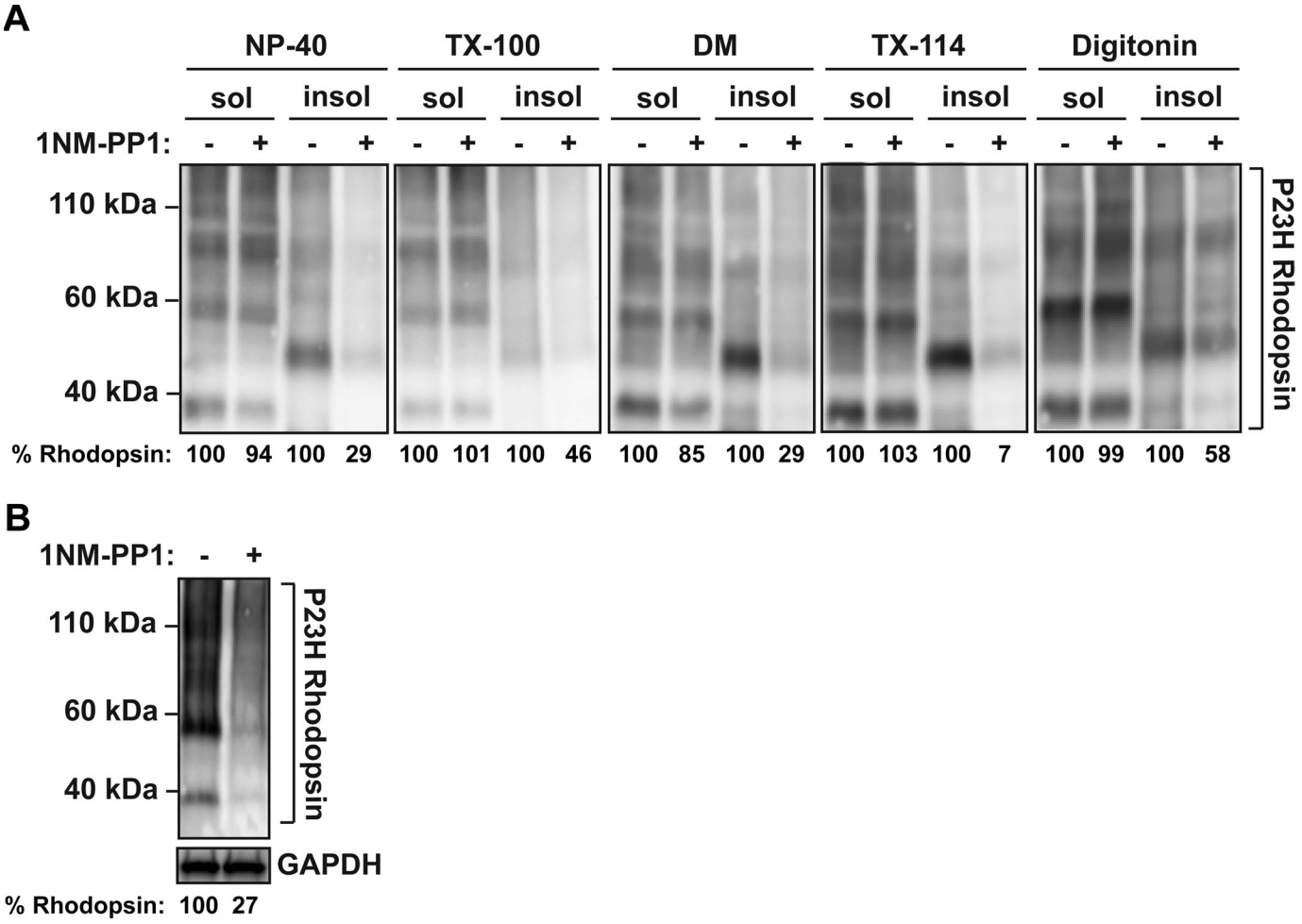

FIGURE 3: IRE1 signaling promotes P23H rhodopsin protein degradation. (A) P23H rhodopsin was expressed in cells bearing IRE1[I642G], and 1NM-PP1 (5 μM) was applied for 24 h. Cell lysates were solubilized in 1% of NP-40, Triton X-100, DM, Triton X-114, or digitonin. Total rhodopsin protein levels from detergent-soluble and -insoluble fractions were detected by immunoblotting and quantified. (B) P23H rhodopsin protein production was induced by application of doxycycline (1 μg/ml) for 30 min in cells bearing tetracycline-inducible P23H rhodopsin and IRE1[I642G]. Doxycycline was removed from media, and when P23H rhodopsin mRNA levels had returned to baseline (~72 h), 1NM-PP1 (5 μM) was applied for 24 h. Total rhodopsin protein levels were detected by immunoblotting and quantified. GAPDH served as a protein loading control.

2 (LAMP2) in immunofluorescence studies compared with cells expressing wild-type rhodopsin (Figure 5A, top two rows), and this colocalization was even more apparent when cells were treated with proteasomal and lysosomal protease inhibitors (Figure 5A, bottom row). These findings suggested that P23H rhodopsin was subjected to lysosomal protein degradation. When we treated cells expressing P23H rhodopsin with bafilomycin, a V-ATPase inhibitor that interrupts autophagosome fusion with lysosomes (Yamamoto *et al.*, 1998), P23H rhodopsin protein levels increased to ~220% of levels seen in untreated cells (Figure 5B). Levels of the lipidated form of light-chain 3 (LC3-II) also increased after bafilomycin treatment (Mizushima and Yoshimori, 2007), confirming the efficacy of bafilomycin in these studies (Figure 5B). These studies indicated that P23H rhodopsin protein degradation also depended on lysosome function through autophagy. Of interest, P23H rhodopsin protein levels decreased in the presence of bafilomycin when IRE1 was activated by1NM-PP1 (Figure 5B and Supplemental Figure S7C). This finding likely reflected the continued proteasomal degradation of P23H rhodopsin when autophagic delivery to lysosome was inhibited.

To test the possibility that P23H rhodopsin protein degradation depended on both lysosome and proteasome, we simultaneously inhibited proteasome and lysosome/autophagy functions and examined effects on P23H rhodopsin protein levels. When we combined lactacystin with bafilomycin, we saw a greater increase in P23H rhodopsin protein levels than with either inhibitor alone (Figure 5C). Similarly, when we combined lactacystin with E64d and pepstatin A, agents that inhibit several lysosomal proteases (McGowan *et al.*, 1989; Mizushima and Yoshimori, 2007), we saw a greater increase in P23H rhodopsin protein levels than with E64d and pepstatin A alone (Figure 5D). Taken together, our results provided evidence that P23H rhodopsin was a substrate for both lysosomal and proteasomal degradation.

IRE1 does not enhance P23H rhodopsin folding and delivery to surface membrane

Chemical and genetic chaperones have been demonstrated to promote P23H rhodopsin exit from the ER by partially ameliorating the misfolding defect (Noorwez *et al.*, 2003, 2004, 2009; Mendes and

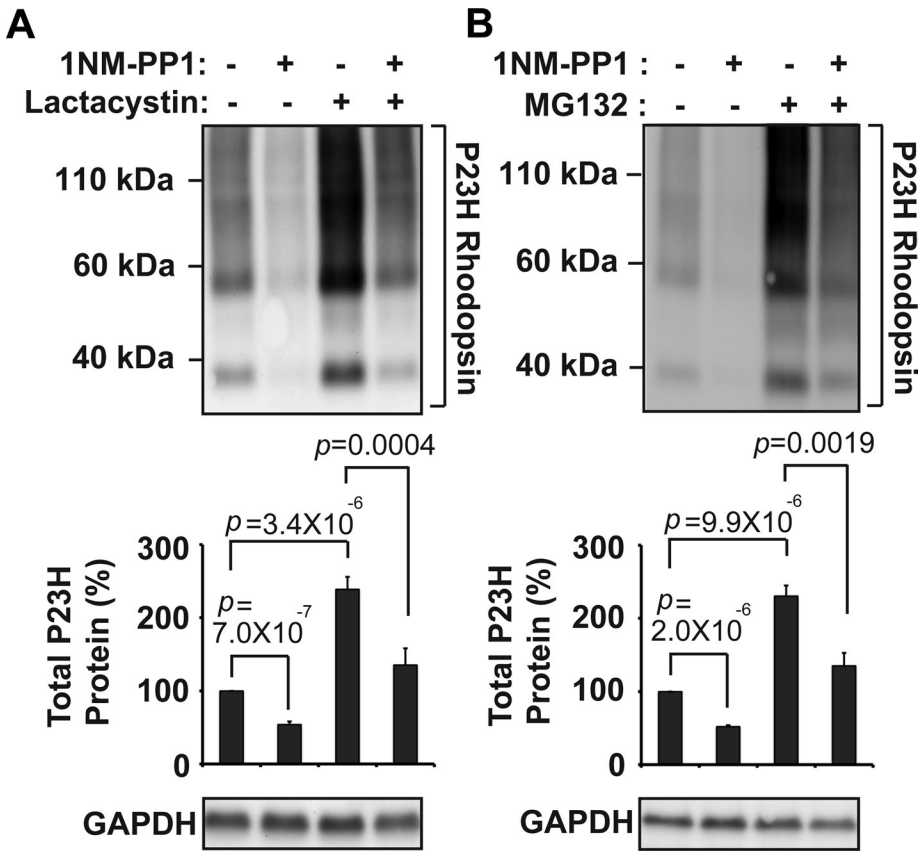

FIGURE 4: P23H rhodopsin protein degradation depends on proteasome function. (A) P23H rhodopsin was expressed in cells bearing IRE1[I642G], and lactacystin (1 μM) and/or 1NM-PP1 (5 μM) was added for 24 h as indicated. Rhodopsin protein levels were detected by immunoblotting and quantified. (B) P23H rhodopsin was expressed in cells bearing IRE1[I642G]. MG132 (1 μM) and/or 1NM-PP1 (5 μM) were applied for 24 h as indicated. (A, B) GAPDH protein levels were assessed as a protein loading control. Immunoblots are representative of three independent experiments. Error bars represent SDs from three experiments. The p values were determined by Student's *t* test analysis.

Cheetham, 2008; Kosmaoglou *et al.*, 2009). The IRE1 signaling pathway transcriptionally upregulates numerous ER chaperones. Therefore we examined whether selective activation of IRE1 could partially restore delivery of P23H rhodopsin to the plasma membrane as another function in addition to promoting P23H rhodopsin protein degradation. When we expressed wild-type rhodopsin in cells bearing IRE1[I642G], we found that rhodopsin was predominantly at the plasma membrane in immunofluorescence studies, and this subcellular localization was not altered upon activation of IRE1 signaling by addition of 1NM-PP1 (Figure 6A). When we expressed P23H rhodopsin in analogous experiments, we found that P23H rhodopsin was retained within the ER, and activation of IRE1[I642G] by addition of 1NM-PP1 did not increase the amount of P23H rhodopsin observed at the plasma membrane in these studies (Figure 6A). Consistent with these imaging studies, when we examined the amount of wild-type and P23H rhodopsin present at the plasma membrane by cell surface biotinylation, we detected large amounts of biotinylated wild-type rhodopsin and minimal P23H rhodopsin at the plasma membrane, and the levels of biotinylated wild-type and P23H rhodopsin were not altered by the addition of 1NM-PP1 (Figure 6B). Therefore our findings demonstrated that IRE1 signaling does not restore P23H rhodopsin delivery to the plasma membrane. Instead, the main effect of IRE1 on P23H rhodopsin in our system was to promote its degradation via the proteasome and lysosome.

Effects of IRE1 on class II rhodopsins and CFTRΔ508

Besides P23H rhodopsin, many additional missense mutations in *rhodopsin* have been identified that cause photoreceptor cell death and vision loss (Berson, 1993). We investigated how IRE1 signaling affected protein levels of five other mutant rhodopsins. When we expressed T17M, Y178C, D190G, K296E, or C185R mutant rhodopsins in cells expressing IRE1[I642G], these mutant rhodopsins formed higher-order multimers and were retained within the ER (Figure 7A; Sung *et al.*, 1991; Saliba *et al.*, 2002; Liu *et al.*, 2010). With addition of 1NM-PP1, we observed reduction in the protein levels of all these mutant rhodopsin proteins that was not seen with wild-type rhodopsin (Figure 7A; reduced to 81% for T17M rhodopsin, 72% for Y178C rhodopsin, 64% for D190G rhodopsin, 49% for K296E rhodopsin, and 83% for C185R rhodopsin after 24 h of drug exposure compared with protein levels in untreated cells). Furthermore, we also observed that these mutant rhodopsins remained predominantly localized in the ER (Supplemental Figure S8). Therefore our results suggested that rhodopsin mutants that cause misfolding were selectively targeted by IRE1 for degradation. Of interest, the magnitude of the reduction in protein levels varied between different rhodopsin mutants for unclear reasons but could reflect differences in the level of protein misfolding and aggregation induced by a particular mutation.

We also asked how IRE1 signaling affected misfolded cystic fibrosis transmembrane conductance regulator (CFTR), a 12-transmembrane ion channel whose loss of function leads to cystic fibrosis. Point mutations in CFTR, such as the CFTRΔF508 mutant, lead to its misfolding and rapid degradation by ERAD (Ward and Kopito, 1994; Farinha and Amaral, 2005; Sun *et al.*, 2006; Younger *et al.*, 2006). By contrast to P23H rhodopsin, CFTRΔ508 does not accumulate as dimers or higher order multimers and instead, is typically found at very low steady-state levels when expressed in cells (Ward and Kopito, 1994; Farinha and Amaral, 2005; Sun *et al.*, 2006; Younger *et al.*, 2006). When we activated IRE1, we did not observe a decrease in CFTRΔF508 protein levels, most likely because its steady-state level was already very low (Figure 8B). These findings indicated that misfolded CFTRΔ508 protein levels were not altered significantly, if at all, by IRE1 signaling in our cell culture system. More broadly, our analysis of multiple mutant rhodopsins and CFTRΔ508 indicated that IRE1 signaling had markedly varying effects on different misfolded membrane proteins.

DISCUSSION

The goal of the present study was to decipher the effects of IRE1 signaling on the fate of the misfolded P23H rhodopsin. A striking effect of IRE1 activation was the sharp drop in the protein levels of misfolded P23H rhodopsin. Intriguingly, the greatest drop was seen with P23H rhodopsin protein present in detergent-insoluble

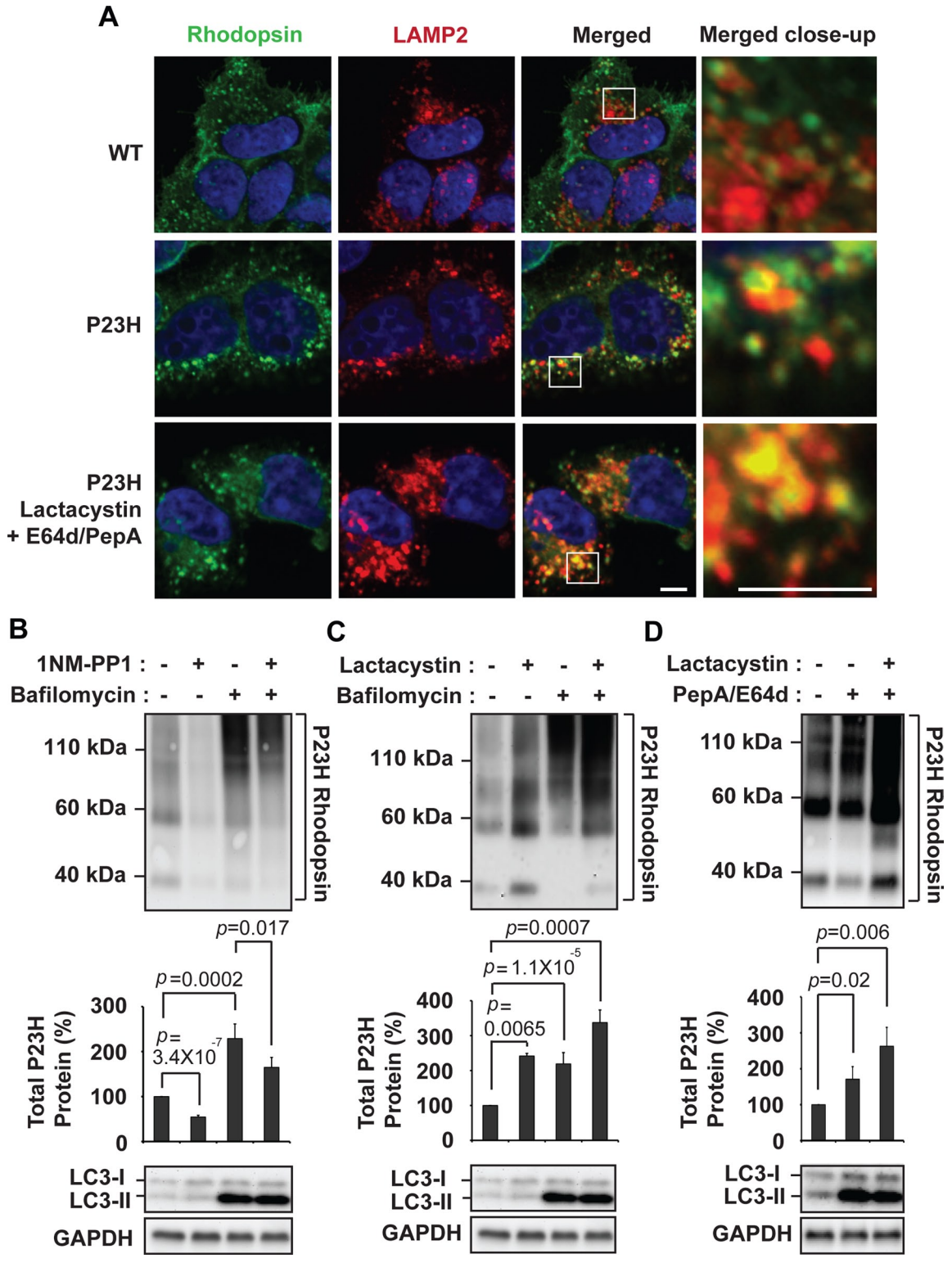

FIGURE 5: P23H rhodopsin protein degradation depends on lysosome function. (A) Wild-type or P23H rhodopsin was expressed in cells, and the subcellular localization of rhodopsin was visualized by immunofluorescence labeling and confocal microscopy (shown in green). The lysosome was visualized by LAMP2 immunostaining (shown in red). The nucleus was visualized by DAPI staining (shown in blue). Magnification bar, 5 μm. (B) P23H rhodopsin was expressed in cells bearing IRE1[I642G], and bafilomycin (1 μM) and/or 1NM-PP1 (5 μM) was added for 20 h as indicated. (C) P23H rhodopsin was expressed in cells, and lactacystin (1 μM) and/or bafilomycin (1 μM) was added for 20 h as indicated. (D) P23H rhodopsin was expressed in cells, and lactacystin (1 μM) and/or E64d (20 μg/ml)/pepstatin A (20 μg/ml) was added for 20 h as indicated. (B–D) Rhodopsin protein levels, LC3-I, and LC3-II protein isoforms were assessed by immunoblotting. GAPDH protein levels were assessed as a protein loading control. Immunoblots are representative of three independent experiments. Error bars represent SDs from three experiments. The p values were determined by Student's *t* test analysis.

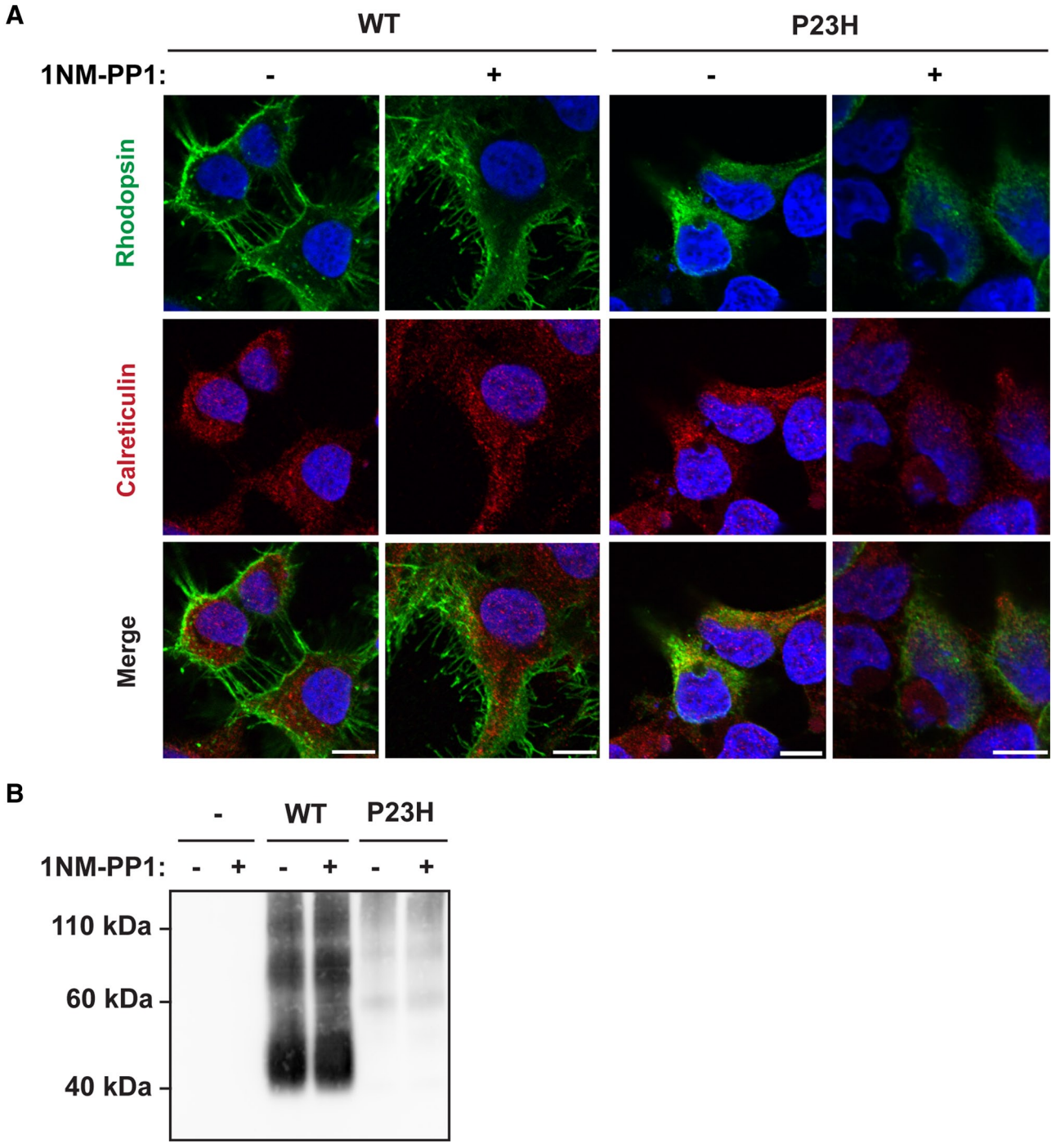

FIGURE 6: IRE1 does not restore the delivery of P23H rhodopsin to the plasma membrane. (A) Wild-type or P23H rhodopsin was expressed in cells bearing IRE1[I642G], and 1NM-PP1 (5 μM) was applied for 24 h as indicated. The subcellular localization of rhodopsin was visualized by immunofluorescence labeling and confocal microscopy (shown in green). The endoplasmic reticulum was visualized by calreticulin immunostaining (shown in red). The nucleus was visualized by DAPI staining (shown in blue). Magnification bars, 10 μm. (B) Wild-type or P23H rhodopsin were expressed in cells bearing IRE1[I642G] with or without application of 1NM-PP1 (5 μM) for 24 h. Surface membrane proteins were biotinylated, and rhodopsin protein levels in the biotinylated fraction were assessed by immunoblotting.

pellet fractions. P23H rhodopsin is highly prone to aggregation, and this aggregated form is likely to comprise much of the P23H rhodopsin protein found in the detergent-insoluble pellet. We envisage several mechanisms to account for the selective reduction in P23H rhodopsin protein levels in pellet fractions after IRE1 activation. First, IRE1 could directly target P23H rhodopsin aggregates for degradation. Second, IRE1 could induce chaperones and enzymes that "solubilize" P23H rhodopsin aggregates, and then this soluble form is degraded. Third, IRE1 could prevent newly synthesized P23H rhodopsin from aggregating and, instead, steer the misfolded protein toward degradation. Many of these mechanisms might be at play, given IRE1's ability to induce numerous genes

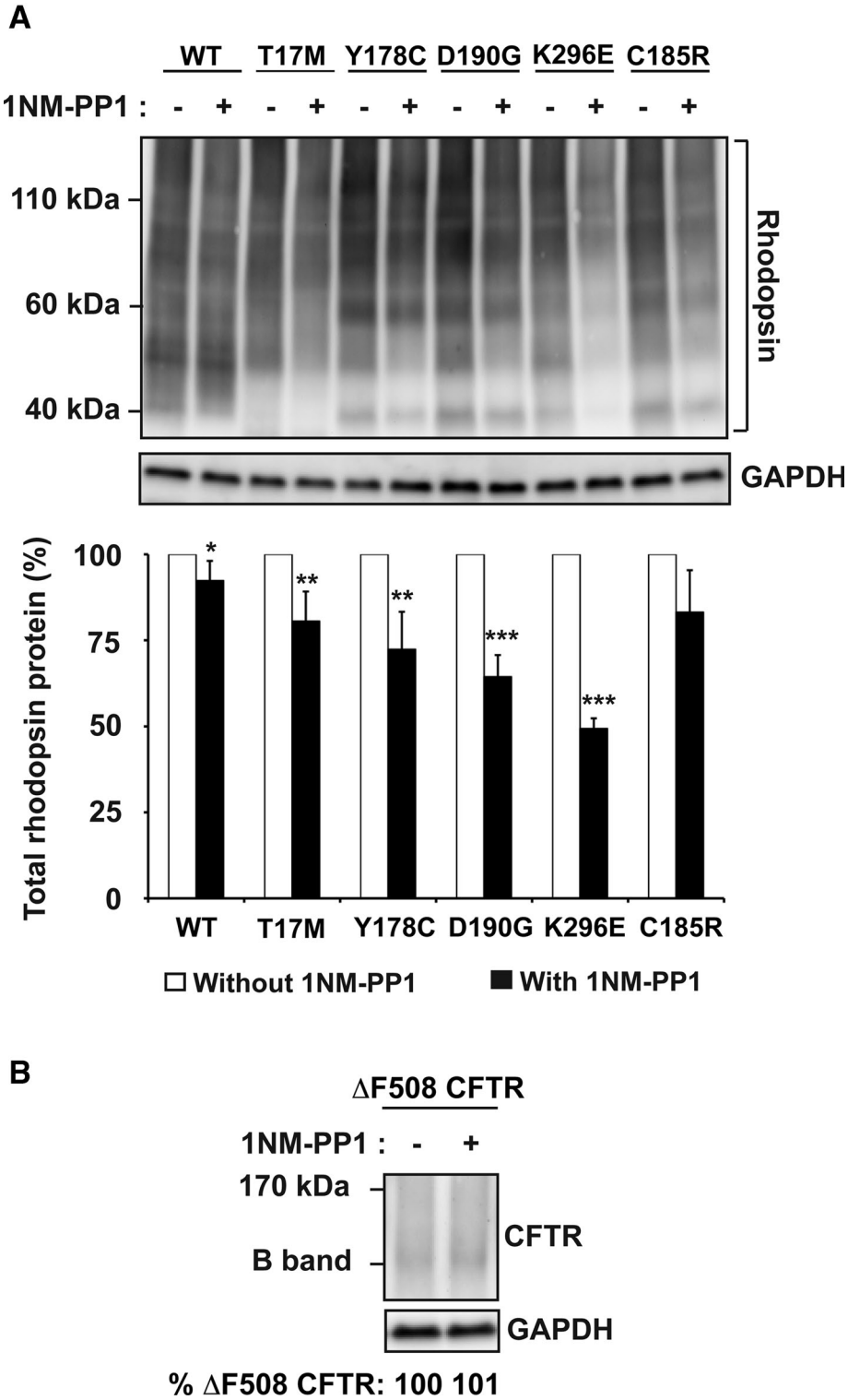

FIGURE 7: (A) Wild-type or mutant T17M, Y178C, D190G, K296E, or C185R rhodopsin was expressed in cells bearing IRE1[I642G], and 1NM-PP1 (5 μM) was applied for 24 h. Total rhodopsin protein levels were detected by immunoblotting and quantified. Error bars represent SDs from three experiments. The p values were determined by Student's *t* test analysis. *p < 0.05, **p < 0.01, ***p < 0.001. (B) CFTRΔF508 was expressed in cells bearing IRE1[I642G], and 1NM-PP1 (5 μM) was applied for 24 h. CFTRΔF508 protein levels were detected by immunoblotting and quantified. (A, B) GAPDH levels were assessed as a protein loading control.

involved in ER protein folding and degradation. Future studies will identify the factors that selectively recognize and target P23H rhodopsin for degradation.

The present study provided evidence that P23H rhodopsin is a substrate for both proteasomal and lysosomal degradation and suggested that the pathways compensated for one another to degrade P23H rhodopsin when one pathway was inhibited (Figure 8). The cellular and molecular events that identify, retrieve, and deliver misfolded membrane proteins for degradation are best understood for ERAD via the proteasome. Recent studies in yeast have proposed a mechanism for ERAD of misfolded membrane proteins that initially entails the recognition of a "bipartite signal" on a misfolded membrane protein comprised of chaperones bound to hydrophobic polypeptides abnormally exposed on the surface of the misfolded protein coupled to lectins bound to modified glycans added through N-linked glycosylation (Kosmaoglou *et al.*, 2008; Buchberger *et al.*, 2010). Then, if the protein-folding problem cannot be corrected, the irretrievably misfolded membrane protein is handed off to a retrotranslocation complex that extracts it from ER membrane for ubiquitinylation and proteasomal degradation in the cytosol (Kawaguchi and Ng, 2007). ERAD components such as EDEM1 and VCP/ter94 have been shown to play important roles in misfolded rhodopsin degradation (Kang and Ryoo, 2009; Kosmaoglou *et al.*, 2009; Griciuc *et al.*, 2010). Of interest, other lectins and ERAD components, such as calnexin, ninaA/peptidyl-prolyl-isomerase, and ninaG/oxidoreductase, are necessary for folding of some rhodopsins but not others (Ahmad *et al.*, 2006; Rosenbaum *et al.*, 2006; Kosmaoglou and Cheetham, 2008; Kosmaoglou *et al.*, 2008). These findings suggest that mutation-specific ERAD cofactors work together with a conserved core ERAD machinery to target P23H rhodopsin for proteasomal degradation. Identifying the full complement of ERAD cofactors specifically targeting human P23H rhodopsin is an important next step.

The role of the lysosome in processing P23H rhodopsin is poorly understood. The present study provided multiple lines of evidence that P23H rhodopsin is a bona fide substrate for lysosomal degradation. However, it is unclear how the cell determines whether to use the proteasome or the lysosome for P23H rhodopsin degradation. P23H rhodopsin readily forms higher-order multimers and aggregates (Figure 1; Illing *et al.*, 2002; Saliba *et al.*, 2002). These aggregates, when arising in the cytosol, could be highly resistant to unfolding and translocation into the 20S proteasome core particle for proteolysis. Furthermore, if P23H rhodopsin aggregates formed while still in the ER membrane, they could overwhelm the ability of ERAD to extract

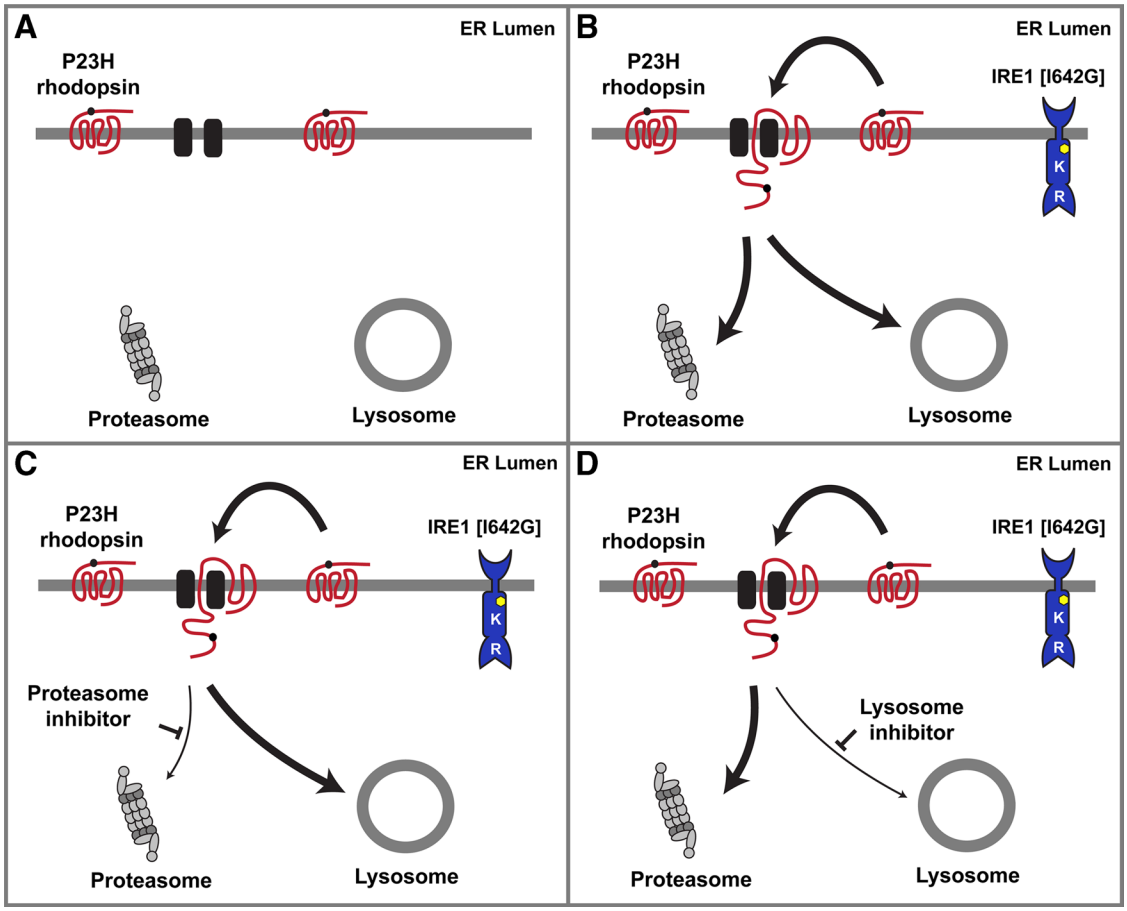

FIGURE 8: Proposed model of P23H rhodopsin protein degradation by IRE1 signaling. (A) P23H rhodopsin is degraded by proteasome and lysosome. (B) IRE1[I642G] activation by 1NM-PP1 enhances P23H rhodopsin degradation. (C) When proteasome function is blocked, IRE1 promotes P23H rhodopsin extraction and degradation by lysosome. (D) When lysosome function is blocked, IRE1 promotes P23H rhodopsin extraction and degradation by proteasome.

and retrotranslocate the misfolded protein for proteasomal degradation. Autophagic recognition of P23H rhodopsin aggregates and delivery to lysosome could enable degradation under these circumstances. Indeed, the autophagy–lysosome system has been implicated in the degradation of a growing number of cytosolic aggregates of misfolded proteins found in neurodegenerative diseases (Rubinsztein, 2006; Winslow and Rubinsztein, 2008; Wong and Cuervo, 2010). More recently, ER-phagy—selective autophagy of ER—has been observed after ER stress and IRE1 activation (Bernales *et al.*, 2006, 2007). ER-phagy could be a mechanism to encapsulate regions of ER containing aggregated P23H rhodopsin for ultimate delivery to the lysosome for degradation. Future studies to identify how IRE1 promotes the degradation of P23H rhodopsin through autophagy/lysosome are required.

Chaperones have shown efficacy in correcting P23H rhodopsin misfolding and enhancing photoreceptor cell survival. Pharmacologic chaperones, such as 11-*cis*-7-ring retinal and 9-*cis*-retinal, can partially correct the P23H rhodopsin misfolding by enhancing its ability to form pigment, acquire mature glycosylation, and transit to the cell surface (Li *et al.*, 1998; Saliba *et al.*, 2002; Noorwez *et al.*, 2003, 2004). Genetic overexpression of EDEM1 in cell culture enhanced P23H rhodopsin degradation and also promoted delivery of P23H rhodopsin to cell surface (Kosmaoglou *et al.*, 2009). The IRE1 signaling pathway upregulates numerous ER protein-folding chaperones, yet we saw no restoration of P23H rhodopsin delivery to the plasma membrane in our studies. This could arise from the concomitant enhancement of P23H rhodopsin protein degradation after IRE1 activation, preventing any "escape" of P23H rhodopsin to plasma membrane. Intriguingly, overexpression of the immunoglobulin-binding protein (BiP)/Grp78 chaperone did not correct P23H rhodopsin misfolding, yet BiP/Grp78 overexpression still enhanced visual function in transgenic animals expressing P23H rhodopsin, in part, by suppressing ER stress-induced proapoptotic signaling pathways in photoreceptors (Gorbatyuk *et al.*, 2010). Chemical-genetic activation of IRE1 in photoreceptors expressing P23H rhodopsin could have similar beneficial effects.

The present findings emphasize the striking ability of IRE1 signaling to remove misfolded P23H rhodopsin from cells while sparing the wild-type counterpart. These findings raise an intriguing question of whether failure of endogenous IRE1 signaling accounts for the toxicity of P23H rhodopsin by allowing its levels to build up to a critical lethal threshold. Genetic studies in lower organisms indicated that the fidelity of protein quality control breaks down as the organism ages (Cuervo and Dice, 2000; David *et al.*, 2010), and recent studies demonstrated that chronic ER stress can render refractive IRE1 signaling required for ER proteostasis (Lin *et al.*, 2007; Li *et al.*, 2010). Determining how chronic stress and/or aging affect IRE1 may reveal why photoreceptors ultimately fail to cope with P23H rhodopsin and die.

Retinitis pigmentosa arising from P23H rhodopsin is emblematic of numerous heritable proteinopathies in which a mutant misfolded protein coexists with the wild-type protein. In many cases, blocking the abnormal protein encoded by the mutated allele is sufficient to restore cell viability because the remaining normal allele encodes sufficient wild-type protein for organismal functions (Lewin *et al*., 1998; LaVail *et al*., 2000). Modulation of IRE1 signaling could be particularly useful in treating these types of proteinopathies by preferentially removing the misfolded protein encoded by the mutated allele while sparing the normal protein encoded by the wild-type allele.

MATERIALS AND METHODS

Cell culture and transfection

HEK293 cells were maintained at 37°C and 5% CO_2 in DMEM (Mediatech, Manassas, VA) supplemented with 10% fetal calf serum (Invitrogen, Carlsbad, CA) and 1% penicillin/streptomycin (Invitrogen). For transient transfection of wild-type rhodopsin, mutant rhodopsins, CFTR, CFTRΔ508, or GFPu, 0.5 μg or indicated amount of plasmids were transfected using Lipofectamine 2000 reagent (Invitrogen) following the manufacturer's instruction. The generation and use of 1NM-PP1–sensitized HEK293 stable cell lines expressing IRE1[I642G] was previously described (Lin *et al*., 2007, 2009). For the construction and selection of tetracycline-inducible wild-type rhodopsin or P23H rhodopsin cell lines, we used the Flp-In T-Rex-293 cell line system (Invitrogen). Briefly, wild-type rhodopsin and the P23H mutant were cloned into the pcDNA5/FRT/TO TOPO TA expression vector (Invitrogen). These plasmids were cotransfected with pCI-neo vector using Lipofectamine 2000 reagent into Flp-In T-Rex-293 cells that were already stably expressing IRE1[I642G]. Two days after transfection, 0.8 mg/ml of G418 (Mediatech) was added to the culture media, and surviving colonies of cells were isolated. To induce the expression of rhodopsin, 1 μg/ml of doxycycline was added to media.

Chemicals

1NM-PP1 was generously provided by C. Zhang and K. Shokat (University of California, San Francisco, CA; Bishop *et al*., 2000). Doxycycline and pepstatin A was obtained from Sigma-Aldrich (St. Louis, MO). Tunicamycin, thapsigargin, bafilomycin, and MG132 were obtained from Calbiochem EMD Bioscience (Darmstadt, Germany). Lactacystin was obtained from Cayman Chemical (Ann Arbor, MI). (2S,3S)-*trans*-Epoxysuccinyl-L-leucylamido-3-methylbutane ethyl ester (E64d) was obtained from Enzo Life Sciences (Plymouth Meeting, PA).

Molecular biology

Cells were lysed and total RNA was collected (RNeasy, Qiagen, Hilden, Germany). PolyA mRNA was reverse transcribed using the SuperScript-RT system (Invitrogen). cDNA was used as template for PCR amplification across the fragment of the *Xbp-1* cDNA bearing the intron target of IRE1 RNAse activity. Primers used included human *Xbp-1*, 5′-TTACGAGAGAAAACTCATGGC-3′ and 5′-GGGTCCAAGTTGTCCAGAATGC-3′. PCR conditions were as follows: 95°C for 5 min; 95°C for 1 min; 58°C for 30 s; 72°C for 30 s; and 72°C for 5 min, with 35 cycles of amplification. PCR products were resolved on a 2.5% agarose/1× Tris-acetate-EDTA gel. Quantification of *Xbp-1* mRNA splicing as a percentage of total *Xbp-1* mRNA was performed using VisionWork LS Software (UVP, Upland, CA).

For quantitative PCR, total RNA was collected from lysed cells (RNeasy). PolyA mRNA was reverse transcribed using the SuperScript-RT system, and aliquots of cDNA were used as template for quantitative PCR. Primers used included human *Rpl19* mRNA, 5′-ATGTATCACAGCCTGTACCTG–3′ and 5′-TTCTTGGTCTCTTCCTCCTTG-3′; and human *rhodopsin* mRNA, 5′- CTTCACCGTCAAGGAGGC-3′ and 5′- GCAAAGAACGCTGGGATG-3′. Quantitative PCR was performed using a Chromo4 DNA Engine (Bio-Rad, Hercules, CA). *Rpl19* mRNA levels, a transcript whose levels are not altered by ER stress, served as an internal normalization standard. PCR conditions were as follows: 95°C for 5 min; 95°C for 10 s; 56.5°C for 10 s; 72°C for 10 s, with 40 cycles of amplification.

Protein biochemistry and quantification

Cells were lysed and homogenized by sonication in ice-cold lysis buffer (1% NP-40, 50 mM Tris-HCl, pH 8, and 150 mM NaCl, containing protease inhibitors [Roche, Basel, Switzerland]). For solubilizing rhodopsin, cells were lysed in ice-cold lysis buffer (1% NP-40, 50 mM Tris-HCl, pH 8, and 150 mM NaCl, containing protease inhibitors [Roche]) and incubated on ice for 30 min. Cell lysates were mixed vigorously every 5 min. Insoluble material was recovered by centrifugation at 15,000 × *g* for 30 min and solubilized in phosphate-buffered saline (PBS) containing 1% SDS for 10 min at room temperature, followed by sonication. Additional lysis buffers used for solubilizing rhodopsin included 1% Triton X-100 (Sigma-Aldrich) in 50 mM Tris-HCl, pH 8, and 150 mM NaCl; 1% DM (Calbiochem EMD Bioscience) in PBS, pH 7.4, 1% Triton X-114 (Sigma-Aldrich) in PBS, pH 7.4, and 1% digitonin (Sigma-Aldrich) in PBS, pH 7.4. Protein concentrations of the total cell lysates, soluble rhodopsin, and insoluble material were determined by BCA Protein Assay Kit (Pierce, Rockford, IL). Five micrograms or the indicated amount of total protein was loaded onto 4–12% SDS–PAGE minigels (NuPAGE, Invitrogen) or 4–15% Mini-PROTEAN TGX precast gels (Bio-Rad) and analyzed by Western blot. The following antibodies and dilutions were used for immunoblotting: anti-rhodopsin at 1:1000 (Santa Cruz Biotechnologies, Santa Cruz, CA); B630N anti-rhodopsin at 1:1000 (a generous gift from W. C. Smith, University of Florida, Gainesville, FL); anti-VCAM1 at 1:1000 (Santa Cruz Biotechnologies); anti–glyceraldehyde 3-phosphate dehydrogenase (GAPDH) at 1:5000 (Santa Cruz Biotechnologies); anti-GFP at 1:5000 (Santa Cruz Biotechnologies); anti-LC3 antibody at 1:1000 (Cell Signaling, Danvers, MA); and anti-CFTR at 1:1000 (Millipore, Billerica, MA). After incubation with primary antibody, membranes were washed in TBS with 0.1% Tween-20 and incubated in horseradish peroxidase–coupled secondary antibody (Amersham, Piscataway, NJ) diluted at 1:5000 in washing buffer with 5% nonfat milk for 1 h. Immunoreactivity was detected using the enhanced chemiluminescence assay (Pierce).

PNGase (New England Biolabs, Ipswich, MA) digestion was performed on total cell lysate for 6 h at 37°C in the buffer supplied by the manufacturer (Supplemental Figure S9).

Protein quantification was measured using VisionWork LS Software. Rhodopsin protein levels were determined by measuring the area density within the bracket (including glycosylated monomers, dimer, and multimers) indicated in the figures after normalizing with the equivalent area density from the control lane.

Protein biotinylation

For cell surface biotinylation, cells were grown in 10-cm dishes coated with poly-D-lysine and transfected with 3 μg of wild-type rhodopsin or mutant P23H rhodopsin. Four hours after transfection, cells were treated with or without 1NM-PP1 for 24 h. The cells were then washed with ice-cold PBS containing 1 mM $MgCl_2$ and 0.1 mM $CaCl_2$. After washing, 5 ml of $NaIO_4$ (Pierce; 10 mM in ice-cold PBS containing 1 mM $MgCl_2$ and 0.1 mM $CaCl_2$) was added to the dishes

and agitated for 30 min at 4°C in the dark. After washing (three times) with PBS containing $MgCl_2$ and $CaCl_2$, the cells were labeled with biotin hydrazide (Pierce; 2 mM in ice-cold PBS containing $MgCl_2$ and $CaCl_2$) at 4°C in the dark. Biotinylated cells were collected and pelleted by brief centrifugation and solubilized in 0.5 ml of ice-cold lysis buffer (1% NP-40, 50 mM Tris-HCl, pH 8, and 150 mM NaCl, containing protease inhibitors [Roche]). Three hundred µl of a 50% slurry of neutrAvidin-agarose beads (Pierce) was incubated with biotinylated cell lysates. The neutrAvidin-agarose beads were washed three times with 0.5 ml of PBS containing protease inhibitor, resuspended in 200 µl of 1× SDS sample buffer, and boiled for 5 min. Aliquots of recovered biotinylated proteins were used for Western blot analysis.

Immunofluorescence and confocal microscopy

Cells were grown on poly-D-lysine-coated glass coverslips and transfected with wild-type or P23H rhodopsin. For immunofluorescence analysis, cells were fixed for 20 min at room temperature in 4% paraformaldehyde in PBS, pH 7.4, washed briefly with PBS, and permeabilized with 0.1% Triton X-100 in PBS. Cells were then washed two times with 1% bovine serum albumen (BSA) in PBS and blocked with 5% goat serum in 1% BSA/PBS for 20 min. The coverslips were then incubated at room temperature for 1 h with the mouse monoclonal anti-rhodopsin antibody (1D4; Santa Cruz Biotechnologies) used at a dilution of 1:2000 and the rabbit polyclonal anti-calreticulin antibody (Assay Designs, Plymouth Meeting, PA) used at a dilution of 1:500 or the rabbit polyclonal anti-LAMP2 antibody (a gift from Minoru Fukuda, Burnham Institute, La Jolla, CA; Carlsson *et al*., 1988) at a dilution of 1:500. After washing in 0.1% BSA in PBS three times, cells were incubated with secondary antibodies. Secondary antibodies included Alexa 488 goat anti-mouse (green) antibody (Molecular Probes, Invitrogen) and Alexa 546 goat anti-rabbit (red) antibody (Molecular Probes), and these were used at a dilution of 1:500. After washing in PBS three times, the cover slips were mounted in ProLong Gold antifade reagent with 4′,6-diamidino-2-phenylindole (DAPI; Invitrogen), and images were collected with a FluoView-1000 confocal microscope (Olympus, Tokyo, Japan) and processed using Olympus FluoView, version 2.0a, Viewer software at the University of California, San Diego, microscopy facility (http://microscopy.ucsd.edu).

Statistical analysis

All results are expressed as mean ± SD of at least three independent experiments. Two-tailed *t* tests were performed to determine p values for paired samples. A value of $p < 0.05$ was considered significant.

ACKNOWLEDGMENTS

We thank W. C. Smith, R. Ayyagari, M. Fukuda, M. Kamps, R. Kopito, K. Shokat, L. Wiseman, and C. Zhang for helpful comments and generous provision of reagents. These studies were supported by the American Federation for Aging Research, the Hope for Vision Foundation, the Karl Kirchgessner Foundation, the University of California, San Diego, Neuroscience Shared Microscopy Facility (P30-NS047101), and National Institutes of Health Grants EY018313 and EY020846. W.-C.C. received postdoctoral support from the Fight-for-Sight Foundation.

REFERENCES

Ahmad ST, Natochin M, Barren B, Artemyev NO, O'Tousa JE (2006). Heterologous expression of bovine rhodopsin in *Drosophila* photoreceptor cells. Invest Ophthalmol Vis Sci 47, 3722–3728.

Bence NF, Sampat RM, Kopito RR (2001). Impairment of the ubiquitin-proteasome system by protein aggregation. Science 292, 1552–1555.

Bernales S, McDonald KL, Walter P (2006). Autophagy counterbalances endoplasmic reticulum expansion during the unfolded protein response. PLoS Biol 4, e423.

Bernales S, Schuck S, Walter P (2007). ER-phagy: selective autophagy of the endoplasmic reticulum. Autophagy 3, 285–287.

Berson EL (1993). Retinitis pigmentosa.. Invest Ophthalmol Vis Sci 34, 1659–1676.

Bishop AC *et al*. (2000). A chemical switch for inhibitor-sensitive alleles of any protein kinase. Nature 407, 395–401.

Buchberger A, Bukau B, Sommer T (2010). Protein quality control in the cytosol and the endoplasmic reticulum: brothers in arms. Mol Cell 40, 238–252.

Calfon M, Zeng H, Urano F, Till JH, Hubbard SR, Harding HP, Clark SG, Ron D (2002). IRE1 couples endoplasmic reticulum load to secretory capacity by processing the XBP-1 mRNA. Nature 415, 92–96.

Carlsson SR, Roth J, Piller F, Fukuda M (1988). Isolation and characterization of human lysosomal membrane glycoproteins, h-lamp-1 and h-lamp-2Major sialoglycoproteins carrying polylactosaminoglycan. J Biol Chem 263, 18911–18919.

Cox JS, Shamu CE, Walter P (1993). Transcriptional induction of genes encoding endoplasmic reticulum resident proteins requires a transmembrane protein kinase. Cell 73, 1197–1206.

Cuervo AM, Dice JF (2000). Age-related decline in chaperone-mediated autophagy. J Biol Chem 275, 31505–31513.

David DC, Ollikainen N, Trinidad JC, Cary MP, Burlingame AL, Kenyon C (2010). Widespread protein aggregation as an inherent part of aging in *C. elegans*. PLoS Biol 8, e1000450.

Dryja TP, McGee TL, Reichel E, Hahn LB, Cowley GS, Yandell DW, Sandberg MA, Berson EL (1990). A point mutation of the rhodopsin gene in one form of retinitis pigmentosa. Nature 343, 364–366.

Eriksson KK, Vago R, Calanca V, Galli C, Paganetti P, Molinari M (2004). EDEM contributes to maintenance of protein folding efficiency and secretory capacity. J Biol Chem 279, 44600–44605.

Farinha CM, Amaral MD (2005). Most F508del-CFTR is targeted to degradation at an early folding checkpoint and independently of calnexin. Mol Cell Biol 25, 5242–5252.

Gonzalez TN, Sidrauski C, Dorfler S, Walter P (1999). Mechanism of non-spliceosomal mRNA splicing in the unfolded protein response pathway. EMBO J 18, 3119–3132.

Gorbatyuk MS, Knox T, LaVail MM, Gorbatyuk OS, Noorwez SM, Hauswirth WW, Lin JH, Muzyczka N, Lewin AS (2010). Restoration of visual function in P23H rhodopsin transgenic rats by gene delivery of BiP/Grp78. Proc Natl Acad Sci USA 107, 5961–5966.

Griciuc A, Aron L, Roux MJ, Klein R, Giangrande A, Ueffing M (2010). Inactivation of VCP/ter94 suppresses retinal pathology caused by misfolded rhodopsin in *Drosophila*. PLoS Genet 6, piie1001075.

Han D, Lerner AG, Vande Walle L, Upton JP, Xu W, Hagen A, Backes BJ, Oakes SA, Papa FR (2009). IRE1alpha kinase activation modes control alternate endoribonuclease outputs to determine divergent cell fates. Cell 138, 562–575.

Harding HP, Zhang Y, Ron D (1999). Protein translation and folding are coupled by an endoplasmic-reticulum-resident kinase. Nature 397, 271–274.

Hargrave PA (2001). Rhodopsin structure, function, and topography. Invest Ophthalmol Vis Sci 42, 3–9.

Hetz C, Glimcher LH (2009). Fine-tuning of the unfolded protein response: assembling the IRE1alpha interactome. Mol Cell 35, 551–561.

Hollien J, Lin JH, Li H, Stevens N, Walter P, Weissman JS (2009). Regulated Ire1-dependent decay of messenger RNAs in mammalian cells. J Cell Biol 186, 323–331.

Hollien J, Weissman JS (2006). Decay of endoplasmic reticulum-localized mRNAs during the unfolded protein response. Science 313, 104–107.

Illing ME, Rajan RS, Bence NF, Kopito RR (2002). A rhodopsin mutant linked to autosomal dominant retinitis pigmentosa is prone to aggregate and interacts with the ubiquitin proteasome system. J Biol Chem 277, 34150–34160.

Iwawaki T, Akai R, Kohno K (2010). IRE1alpha disruption causes histological abnormality of exocrine tissues, increase of blood glucose level, and decrease of serum immunoglobulin level. PLoS One 5, e13052.

Kang MJ, Ryoo HD (2009). Suppression of retinal degeneration in *Drosophila* by stimulation of ER-associated degradation. Proc Natl Acad Sci USA 106, 17043–17048.

Kaushal S (2006). Effect of rapamycin on the fate of P23H opsin associated with retinitis pigmentosa (an American Ophthalmological Society thesis). Trans Am Ophthalmol Soc 104, 517–529.

Kaushal S, Khorana HG (1994). Structure and function in rhodopsin. 7. Point mutations associated with autosomal dominant retinitis pigmentosa. Biochemistry 33, 6121–6128.
Kawaguchi S, Ng DT (2007). SnapShot: ER-associated protein degradation pathways. Cell 129, 1230.
Kosmaoglou M, Cheetham ME (2008). Calnexin is not essential for mammalian rod opsin biogenesis. Mol Vis 14, 2466–2474.
Kosmaoglou M, Kanuga N, Aguila M, Garriga P, Cheetham ME (2009). A dual role for EDEM1 in the processing of rod opsin. J Cell Sci 122, 4465–4472.
Kosmaoglou M, Schwarz N, Bett JS, Cheetham ME (2008). Molecular chaperones and photoreceptor function. Prog Retin Eye Res 27, 434–449.
LaVail MM, Yasumura D, Matthes MT, Drenser KA, Flannery JG, Lewin AS, Hauswirth WW (2000). Ribozyme rescue of photoreceptor cells in P23H transgenic rats: long-term survival and late-stage therapy. Proc Natl Acad Sci USA 97, 11488–11493.
Lee AH, Iwakoshi NN, Glimcher LH (2003). XBP-1 regulates a subset of endoplasmic reticulum resident chaperone genes in the unfolded protein response. Mol Cell Biol 23, 7448–7459.
Lewin AS, Drenser KA, Hauswirth WW, Nishikawa S, Yasumura D, Flannery JG, LaVail MM (1998). Ribozyme rescue of photoreceptor cells in a transgenic rat model of autosomal dominant retinitis pigmentosa. Nat Med 4, 967–971.
Li H, Korennykh AV, Behrman SL, Walter P (2010). Mammalian endoplasmic reticulum stress sensor IRE1 signals by dynamic clustering. Proc Natl Acad Sci USA 107, 16113–16118.
Li T, Sandberg MA, Pawlyk BS, Rosner B, Hayes KC, Dryja TP, Berson EL (1998). Effect of vitamin A supplementation on rhodopsin mutants threonine-17 –> methionine and proline-347 –> serine in transgenic mice and in cell cultures. Proc Natl Acad Sci USA 95, 11933–11938.
Lin JH, Li H, Yasumura D, Cohen HR, Zhang C, Panning B, Shokat KM, LaVail MM, Walter P (2007). IRE1 signaling affects cell fate during the unfolded protein response. Science 318, 944–949.
Lin JH, Li H, Zhang Y, Ron D, Walter P (2009). Divergent effects of PERK and IRE1 signaling on cell viability. PLoS ONE 4, e4170.
Liu H, Wang M, Xia CH, Du X, Flannery JG, Ridge KD, Beutler B, Gong X (2010). Severe retinal degeneration caused by a novel rhodopsin mutation. Invest Ophthalmol Vis Sci 51, 1059–1065.
McGowan EB, Becker E, Detwiler TC (1989). Inhibition of calpain in intact platelets by the thiol protease inhibitor E-64d. Biochem Biophys Res Commun 158, 432–435.
Mendes HF, Cheetham ME (2008). Pharmacological manipulation of gain-of-function and dominant-negative mechanisms in rhodopsin retinitis pigmentosa. Hum Mol Genet 17, 3043–3054.
Mizushima N, Yoshimori T (2007). How to interpret LC3 immunoblotting. Autophagy 3, 542–545.
Noorwez SM, Kuksa V, Imanishi Y, Zhu L, Filipek S, Palczewski K, Kaushal S (2003). Pharmacological chaperone-mediated in vivo folding and stabilization of the P23H-opsin mutant associated with autosomal dominant retinitis pigmentosa. J Biol Chem 278, 14442–14450.
Noorwez SM, Malhotra R, McDowell JH, Smith KA, Krebs MP, Kaushal S (2004). Retinoids assist the cellular folding of the autosomal dominant retinitis pigmentosa opsin mutant P23H. J Biol Chem 279, 16278–16284.
Noorwez SM, Sama RR, Kaushal S (2009). Calnexin improves the folding efficiency of mutant rhodopsin in the presence of pharmacological chaperone 11-*cis*-retinal. J Biol Chem 284, 33333–33342.
Oikawa D, Tokuda M, Iwawaki T (2007). Site-specific cleavage of CD59 mRNA by endoplasmic reticulum-localized ribonuclease, IRE1. Biochem Biophys Res Commun 360, 122–127.
Olivari S, Galli C, Alanen H, Ruddock L, Molinari M (2005). A novel stress-induced EDEM variant regulating endoplasmic reticulum-associated glycoprotein degradation. J Biol Chem 280, 2424–2428.
Olsson JE, Gordon JW, Pawlyk BS, Roof D, Hayes A, Molday RS, Mukai S, Cowley GS, Berson EL, Dryja TP (1992). Transgenic mice with a rhodopsin mutation (Pro23His): a mouse model of autosomal dominant retinitis pigmentosa. Neuron 9, 815–830.
Ron D, Walter P (2007). Signal integration in the endoplasmic reticulum unfolded protein response. Nat Rev Mol Cell Biol 8, 519–529.
Rosenbaum EE, Hardie RC, Colley NJ (2006). Calnexin is essential for rhodopsin maturation, Ca2+ regulation, and photoreceptor cell survival. Neuron 49, 229–241.
Rubinsztein DC (2006). The roles of intracellular protein-degradation pathways in neurodegeneration. Nature 443, 780–786.
Sakami S, Maeda T, Bereta G, Okano K, Golczak M, Sumaroka A, Roman AJ, Cideciyan AV, Jacobson SG, Palczewski K (2011). Probing mechanisms of photoreceptor degeneration in a new mouse model of the common form of autosomal dominant retinitis pigmentosa due to P23H opsin mutations. J Biol Chem 286, 10551–10567.
Saliba RS, Munro PM, Luthert PJ, Cheetham ME (2002). The cellular fate of mutant rhodopsin: quality control, degradation and aggresome formation. J Cell Sci 115, 2907–2918.
Sun F, Zhang R, Gong X, Geng X, Drain PF, Frizzell RA (2006). Derlin-1 promotes the efficient degradation of the cystic fibrosis transmembrane conductance regulator (CFTR) and CFTR folding mutants. J Biol Chem 281, 36856–36863.
Sung CH, Schneider BG, Agarwal N, Papermaster DS, Nathans J (1991). Functional heterogeneity of mutant rhodopsins responsible for autosomal dominant retinitis pigmentosa. Proc Natl Acad Sci USA 88, 8840–8844.
Urano F, Wang X, Bertolotti A, Zhang Y, Chung P, Harding HP, Ron D (2000). Coupling of stress in the ER to activation of JNK protein kinases by transmembrane protein kinase IRE1. Science 287, 664–666.
Ward CL, Kopito RR (1994). Intracellular turnover of cystic fibrosis transmembrane conductance regulatorInefficient processing and rapid degradation of wild-type and mutant proteins. J Biol Chem 269, 25710–25718.
Winslow AR, Rubinsztein DC (2008). Autophagy in neurodegeneration and development. Biochim Biophys Acta 1782, 723–729.
Wong E, Cuervo AM (2010). Autophagy gone awry in neurodegenerative diseases. Nat Neurosci 13, 805–811.
Yamamoto A, Tagawa Y, Yoshimori T, Moriyama Y, Masaki R, Tashiro Y (1998). Bafilomycin A1 prevents maturation of autophagic vacuoles by inhibiting fusion between autophagosomes and lysosomes in rat hepatoma cell line, H-4-II-E cells. Cell Struct Funct 23, 33–42.
Yoshida H, Matsui T, Hosokawa N, Kaufman RJ, Nagata K, Mori K (2003). A time-dependent phase shift in the mammalian unfolded protein response. Dev Cell 4, 265–271.
Yoshida H, Matsui T, Yamamoto A, Okada T, Mori K (2001). XBP1 mRNA is induced by ATF6 and spliced by IRE1 in response to ER stress to produce a highly active transcription factor. Cell 107, 881–891.
Younger JM, Chen L, Ren HY, Rosser MF, Turnbull EL, Fan CY, Patterson C, Cyr DM (2006). Sequential quality-control checkpoints triage misfolded cystic fibrosis transmembrane conductance regulator. Cell 126, 571–582.
Zhang K *et al*. (2011). The unfolded protein response transducer IRE-1alpha prevents ER stress-induced hepatic steatosis. EMBO J 30, 1357–1375.
Zhang K, Wong HN, Song B, Miller CN, Scheuner D, Kaufman RJ (2005). The unfolded protein response sensor IRE1alpha is required at 2 distinct steps in B cell lymphopoiesis. J Clin Invest 115, 268–281.